THE ASTROPHYSICAL JOURNAL, 453:384–392, 1995 November 1

APERTURE SYNTHESIS ^{12}CO AND ^{13}CO OBSERVATIONS OF DM TAURI: 350 AU RADIUS CIRCUMSTELLAR GAS DISK

M. SAITO,[1,2,3] R. KAWABE,[1] M. ISHIGURO,[1] S. M. MIYAMA,[4] M. HAYASHI,[4] T. HANDA,[5] Y. KITAMURA,[6,7] AND T. OMODAKA[8]

Received 1994 July 28; accepted 1995 May 4

ABSTRACT

We have made aperture synthesis observations of ^{12}CO (1–0), ^{13}CO (1–0), 2.6 mm, and 2.7 mm continuum emissions from a young star DM Tau with the Nobeyama Millimeter Array (NMA). It has been found from our observations that ^{12}CO gas with a size of 5.″9 × 4.″6 is associated with DM Tau and the systematic velocity gradient of ^{12}CO exists along P.A. = 160°. The observational results suggest that DM Tau is surrounded by the disk structure of molecular gas ("circumstellar gas disk") with a radius of 350 AU and an inclination of 40° and that the kinematics of the disk is consistent with Keplerian rotation around DM Tau with a mass of 0.48 $M_\odot$. We have also detected the ^{13}CO, 2.6 mm, and 2.7 mm continuum emissions from the disk around DM Tau. The H_2 mass of the gas disk in the outer region ($r > 100$ AU) is estimated to be 2.3×10^{-3} $M_\odot$ from the ^{12}CO and ^{13}CO emissions, and that in the inner region ($r < 100$ AU) is 0.019 $M_\odot$ from 2.6 mm continuum flux. Although the disk around DM Tau is larger than the solar system, the disk may be a protoplanetary disk from the viewpoint that the mass of the disk is comparable to the minimum mass of the solar nebula ($\sim$0.01 $M_\odot$) and the kinematics of the disk is consistent with Keplerian rotation. The radial dependence of H_2 gas surface density of the disk is roughly estimated as $\Sigma(r) \propto r^{-2.0\pm0.3}$ using the outer and the inner masses of the disk, unless the depletion of ^{13}CO occurs in the outer region. This power-law index of 2.0 ± 0.3 is significantly larger than the value of 1.5 adopted in the model of minimum solar nebula (Kyoto model).

DM Tau is one of the young stars located in the L1551 star-forming region, including HL Tau, GG Tau, and a protostar, L1551–IRS 5. The systemic velocities of gas disks found around these stars in the different evolutional stages are in the very narrow range ($V_{LSR} = 5.7 - 6.4$ km s^{-1}), and the major axes of the disks are roughly perpendicular to the direction of the local magnetic field. It is likely that these stars were successively formed in the same parent cloud and that the magnetic field might play an important role in the formation of the star-disk systems.

Subject headings: stars: circumstellar matter — stars: formation — stars: pre–main-sequence

1. INTRODUCTION

Observational studies of circumstellar environments around protostars and T Tauri stars are very important in order to investigate external planetary systems and the process of planet formation as well as the process of star formation. In the process of star formation from a collapsing cloud with some angular momentum, a rotating disk of gas and dust is thought to be formed around a protostar and remains in the following young star phase. Such a disk structure, the so-called protoplanetary disk, is expected to have a size comparable to the solar system. Cameron (1985) suggests that a massive disk (~ 1 $M_\odot$) has a gravitational instability and begins to fragment into many parts, some of which will become planets (e.g., Miyama et al. 1995). The Kyoto model (Hayashi, Nakazawa, & Nakagawa 1985) and the Safronov model (Sagronov & Ruzmaikina 1985) proposed that the mass of the protoplanetary disk is small ($\sim$0.01 $M_\odot$) and the planets are formed by collision and growth of planetesimals. Hence, to determine the mass of the disk around young stellar objects is very important to select the formation scenario of planets.

In the 1980s, the rapid advance in astrophysical technology, i.e., the *IRAS* satellite, millimeter wave interferometers, and sensitive bolometers, motivated us to challenge the observations of circumstellar environments around young stars. In the nearby star-forming regions like Taurus, ρ Ophiuchi, and Chameleon, it was shown from many observations and analyses that T Tauri stars have continuum excess in the IR wavelength (Rucinski 1985; Strom et al. 1989; Cohen, Emerson, & Beichman 1989), and it was suggested that these infrared excesses in T Tauri stars are caused by emission from dust grains of the circumstellar disk surrounding those stars. The millimeter continuum surveys were performed in view of the evolution of dust disk (Adams, Emerson, & Fuller 1990; Beckwith et al. 1990, hereafter BSCG; Andre & Montmerle 1994; Henning et al. 1993). It was concluded from their observations that about half of all T Tauri stars have cold dusty disks with masses of 0.001–1 $M_\odot$. The 3 mm continuum obser-

[1] Nobeyama Radio Observatory, Nobeyama, Minamimaki, Minamisaku, Nagano 384-13, Japan. Nobeyama Radio Observatory (NRO) is a branch of the National Astronomical Observatory.
[2] Department of Astronomy, School of Science, University of Tokyo, 3-7-1, Hongo, Bunkyo, Tokyo 113, Japan.
[3] masao@nro.nao.ac.jp.
[4] National Astronomical Observatory, 2-11-1, Oosawa, Mitaka, Tokyo 181, Japan.
[5] Institute of Astronomy, Faculty of Science, University of Tokyo, 2-11-1, Oosawa, Mitaka, Tokyo 181, Japan.
[6] Department of Liberal Arts, School of Allied Medical Sciences, Kagoshima University, 8-35-1, Sakuragaoka, Kagoshima 890, Japan.
[7] Present address: Institute of Space and Astronautical Science, 3-1-1 Yoshinodai, Sagamihara, Kanagawa 229, Japan.
[8] Department of Physics, College of Liberal Arts, Kagoshima University, 1-21-3, Korimoto, Kagoshima 890, Japan.

vations of young stellar objects with the Nobeyama Millimeter Array (NMA) suggest that compact and highly dense disks may be formed in the course of the evolution of central stars from embedded sources to T Tauri stars (Ohashi et al. 1991, hereafter OKHI). In aperture synthesis observations in CO emissions, it was found that several T Tauri stars have gaseous disk structures (HL Tau, DG Tau, GG Tau; Sargent & Beckwith 1991; Sargent & Beckwith 1989; Kawabe et al. 1993). ^{13}CO observations with NMA (Hayashi, Ohashi, & Miyama 1993, hereafter HOM) revealed the existence of a dynamically accreting disk with a radius of 1400 AU around HL Tau. Recent ^{13}CO observations show that the 3000 AU scale dispersing gaseous disk exists around DG Tau (Kitamura, Kawabe, & Saito 1995). Above all, it is remarkable that the circumstellar gaseous disk found by Kawabe et al. (1993) around GG Tau has a Keplerian rotating motion and a more compact size, $r \sim 500$ AU. Synthesis observations of GG Tau in ^{13}CO with high resolution (Dutrey, Guilloteau, & Simon 1994) confirmed a rotating gaseous ring around the star and revealed that the disk has an inner cavity with a radius of 180 AU. This inner cavity is predicted by Kawabe et al. (1993) because GG Tau is a binary system. It has not been reported that the compact rotating gaseous disk exists around a single star except GM Aur (Koerner, Sargent, & Beckwith 1993).

DM Tau is one of the classical T Tauri stars in the Taurus region at the distance of 140 pc (Elias 1978) and is not a binary system in the systematic search for young binaries in Taurus (Leinert et al. 1993). Relatively strong 1.3 mm continuum was detected toward DM Tau (109 mJy) by BSCG. Recently ^{12}CO and ^{13}CO emissions were detected toward DM Tau using the Nobeyama 45 m telescope (Handa et al. 1995). The ^{12}CO profile maps show that there exists CO emission which is associated with DM Tau in both position and velocity. The ^{13}CO profile toward DM Tau shows a symmetric double peak, suggesting a Keplerian rotating disk. The center velocity of ^{12}CO emission, 5.9 km s^{-1} in LSR, coincides with the reported radial velocity for DM Tau and is different from that of the background cloud ($V_{LSR} = 9$ km s^{-1}). The disk size was estimated to be about 1000 AU using a Keplerian disk model, but it was impossible to resolve the structure and to obtain the kinematics and inclination of the gas disk from their observations. We have made aperture synthesis ^{12}CO and ^{13}CO observations with the NMA in order to investigate the structure and kinematics of the molecular gas associated with DM Tau. In this paper we adopted the stellar mass and age as 0.48 $M_\odot$ and 1.0×10^6 yr; these are the estimated values in Handa et al. (1995).

2. OBSERVATIONS

We observed DM Tau in the ^{12}CO ($J = 1$–0) line with the NMA between 1992 December and 1994 March. The ^{12}CO observations were made with two different antenna configurations. Projected baselines ranged from 5 kλ to 60 kλ. The synthesized beam was $6''.5 \times 4''.9$ at P.A. = 149°. The stellar position of DM Tau is R.A.(1950) = $4^h30^m54^s.7$, decl.(1950) = 18°03′56″.7 (Herbig & Robbin-Bell 1988). Our observations are insensitive to the structures extended more than 40″ because the minimum projected baseline length is 5 kλ. The primary beam size (field of view) was about 65″ (FWHM). We also observed DM Tau in the ^{13}CO line ($J = 1$–0) between 1993 April and May. The synthesized beam was $7''.0 \times 3''.9$ at P.A. = 153°.

We use the superconductor-insulator-superconductor receivers (Sunada, Kawabe, & Inatani 1993), and the typical system noise temperatures in single-sideband were ~600 K and ~500 K at the zenith at 2.6 mm and 2.7 mm, respectively. The back end was the fast Fourier transform spectrocorrelator FX (Chikada et al. 1987) with 1024 channels per baseline with a bandwidth of 320 MHz. The velocity resolution of the ^{12}CO line is about 0.81 km s^{-1}, and that of the ^{13}CO line is about 0.85 km s^{-1}. The line free channels of the FX correlator in the ^{12}CO and ^{13}CO observations were used for the mapping of continuum emission at 2.6 mm and 2.7 mm. We used 3C 273 as a bandpass calibrator and used 0420−014 in 1993 and 0528+134 in 1994 as a phase and gain calibrator for the observations. The flux scales of 0420−014 and 0528+134 were derived by the observations of planets. The flux density of 0420−014 at 98 GHz (3.0 mm) changed from 4.0 Jy to 2.1 Jy between 1992 December and 1993 March, and that of 0528+134 was 4.8 Jy in 1994 March. The overall flux uncertainty is about 20%.

All maps for the ^{12}CO, ^{13}CO, 2.6 mm, and 2.7 mm continuum emissions were made using the CLEAN algorithm by the NRAO[9] Astronomical Image Processing System (AIPS). The absolute positional accuracy in the maps is estimated to be better than 1″.5 by taking into account the baseline error and atmospheric phase fluctuation, and the relative positional accuracy of line maps to continuum is better than 0″.5. The rms noise in the 2.6 mm continuum map was 7 mJy beam^{-1}, and in the 2.7 mm continuum map it was 8 mJy beam^{-1}. The rms noise in ^{12}CO channel maps with a velocity width of 0.81 km s^{-1} was 180 mJy beam^{-1}, and that in ^{13}CO channel maps with a velocity width of 0.85 km s^{-1} was 220 mJy beam^{-1}.

3. RESULTS

3.1. ^{12}CO (1–0) *Emission*

Figure 1 shows velocity channel maps of ^{12}CO emission from DM Tau for velocities from $V_{LSR} = 3.5$ km s^{-1} to 7.6 km s^{-1} with a velocity resolution of 0.81 km s^{-1}. The synthesized beam was $6''.5 \times 4''.9$ at P.A. = 149°. The line emission of ^{12}CO was detected just toward the young star DM Tau for channels from $V_{LSR} = 4.4$ km s^{-1} to $V_{LSR} = 6.8$ km s^{-1} at 4–8 σ levels. No significant emission with the star was detected out of this velocity range. The flux density of the peak emission in our channel maps was 1.4 Jy (4.1 K in T_B) at $V_{LSR} = 5.2$ km s^{-1}. Since the structure is not perfectly resolved by the synthesized beam, the excitation temperature, T_{ex}, is larger than $T_B + T_{BB}(2.7\text{ K}) = 6.8$ K.

The mean of V_{LSR} weighted by the ^{12}CO intensity is estimated to be 5.7 ± 0.2 km s^{-1} from the channel maps. The ^{12}CO mean velocity, $V_{LSR} = 5.7$ km s^{-1}, is consistent with both the ^{12}CO systemic velocity, $V_{LSR} = 5.9$ km s^{-1}, and the ^{13}CO systemic velocity, $V_{LSR} = 5.7$ km s^{-1} obtained with the 45 m telescope (Handa et al. 1995). Hereafter, we use $V_{LSR} = 5.7$ km s^{-1} as the systemic velocity of molecular gas associated with DM Tau.

Figure 2*a* shows a map of the ^{12}CO intensity integrated over the velocity range from $V_{LSR} = 4.0$–7.3 km s^{-1}. The peak position of the ^{12}CO emission coincides with the stellar position by the optical observations (Herbig & Robbin-Bell 1988) within error bars. The map clearly shows that the compact gas structure is associated with the central star. The distribution of the ^{12}CO emission is larger compared to the beam size and is

[9] The National Radio Astronomy Observatory is operated by Associated Universities Inc., under contract with the National Science Foundation.

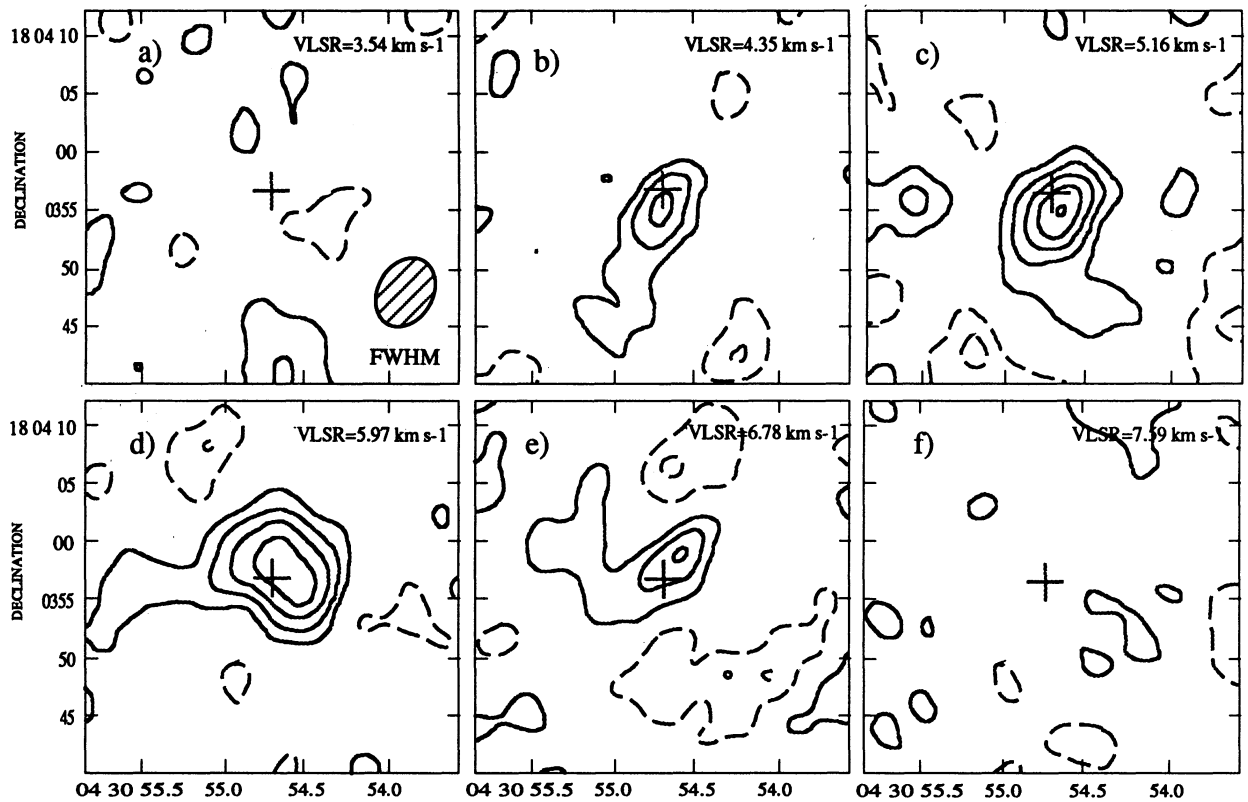

FIG. 1.—(*a–f*) Velocity channel maps of ^{12}CO emission of DM Tau for velocity over V_{LSR} = 3.5–7.6 km s^{-1}. The center velocity of each channel with 0.81 km s^{-1} width is shown in each panel. A cross indicates the optical stellar position. The contour interval is 270 mJy beam^{-1} corresponding to 1.5 σ. A contour with a negative level is indicated with a dashed line.

therefore slightly extended. The beam deconvolved size of the molecular gas distribution in the total ^{12}CO map is obtained to be 5.″9 × 4.″6 (830 AU × 640 AU) at P.A. = 57°. The total flux density is obtained to be 4.8 Jy km s^{-1}.

It is found from Figures 1*b*–1*e* that there exists a systematic velocity gradient of ^{12}CO emission over V_{LSR} = 4.4–6.8 km s^{-1} along the line from southeast to northwest. The peaks of blue- and redshifted emission shift by 2.″5 (corresponding to ~350 AU) with respect to the stellar position (Figs. 1*b*, 1*e*). Figure 2*b* shows the superposition of the blue and red components integrated over V_{LSR} = 4.0–5.6 km s^{-1} and V_{LSR} = 5.6–7.3 km s^{-1}, respectively. Those components are distributed symmetrically in respect to the star, and the blue emission shifts to about 2″ northwest and the red emission shifts to 2″ (corresponding to ~280 AU) southeast of the stellar position. We estimated that the P.A. of the velocity structure is 160° from the two peaks of the blue and red components in Figure 2*b*.

The velocity structure in the ^{12}CO channel maps and the compact structure of the ^{12}CO emission in the total map suggest that DM Tau is surrounded by a rotating circumstellar disk with a radius of hundreds AU. Disk parameters are estimated in § 4.1.

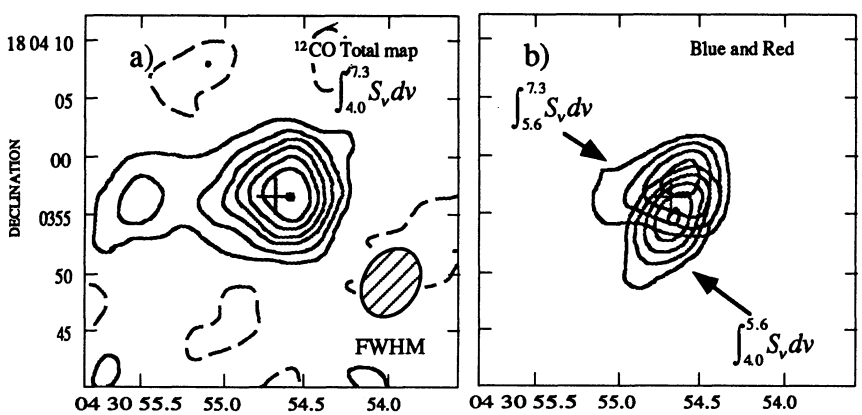

FIG. 2.—(*a*) A map of total integrated ^{12}CO emission over V_{LSR} = 4.0–7.3 km s^{-1} (Fig. 1*b*–1*e*). The contour interval is 150 mJy beam^{-1}. A cross indicates the stellar position. (*b*) A map of the superposition of the blue and red component integrated over two channels (V_{LSR} = 4.0–5.6 km s^{-1} and V_{LSR} = 5.6–7.3 km s^{-1}), respectively. The contour level starts at 3 σ, and the contour interval is 180 mJy corresponding to 1.5 σ.

3.2. ^{13}CO (1–0) *Emission*

Figure 3 shows velocity channel maps of ^{13}CO emission from V_{LSR} = 4.3–7.7 km s^{-1} with the synthesized beam 7.″0 × 3.″9 at P.A. = 153°. We detected significant ^{13}CO emission only at a velocity of V_{LSR} = 5.95 km s^{-1} close to the systemic velocity (Fig. 3*c*). The peak flux density in our 0.85 km s^{-1} resolution maps was 0.7 Jy beam^{-1}, corresponding to 2.7 K in T_B.

Figure 3*f* shows a map of total intensity of ^{13}CO integrated over the velocity range 4.7–7.2 km s^{-1} that is the almost same range as that for which ^{12}CO emission is detected. The ^{13}CO emission at the 3 σ level is clearly centered on the stellar position. This component is unresolved in our 7.″0 × 3.″9 beam. From our ^{13}CO map, the total flux is obtained to be 1.5 Jy km s^{-1}. The ^{13}CO to ^{12}CO flux ratio is estimated to be about 0.3 ± 0.15. If we assume $\tau_{12} = 89\tau_{13}$, τ_{13} is estimated to be 0.4 ± 0.15, where τ_{12} and τ_{13} are the optical depths for ^{12}CO and ^{13}CO lines, respectively.

3.3. 2.6 mm *and* 2.7 mm *Continuum Emission*

We show the 2.6 mm and 2.7 mm continuum maps in Figure 4. We detected 3 σ level continuum emission from DM Tau at 2.6 mm (Fig. 4, *left panel*). The synthesized beam was 5.″4 × 4.″4 at P.A. = 162°. The total integrated flux density in the map is 23 ± 7 mJy. The peak position of the map is at R.A.(1950) = 04^{h}30^{m}54^s.6, decl.(1950) = +18°03′55″ and coincides with the stellar position within positional error as a result of the low signal-to-noise ratio in the map. The distribution of the continuum emission is unresolved with our 5.″4 × 4.″4 beam. We have also detected continuum emission toward DM Tau at 2.7 mm (Fig. 4, *right panel*), and the total flux density in the map is 27 ± 8 mJy. This value is consistent with that at 2.6 mm within error bars.

The frequency dependence of the mass opacity coefficient, κ_ν, is usually assumed to follow a power law, $\kappa_\nu \propto \nu^\beta$. The spectral index, β, is estimated to be 0.22 ± 0.6 from the 2.6 mm total flux, 23 ± 7 mJy, and the 1.3 mm total flux, 109 ± 10 mJy (BSCG). This value is consistent with β, 0.35 ± 0.21, estimated in the submillimeter region within error bars (Beckwith & Sargent 1991). The obtained index, 0.22 ± 0.6, is lower than that obtained for the interstellar normal value, $\beta = 2$. As pointed out by Miyake & Nakagawa (1993), the lower β is explained by the growth of dust particles in the disk because the density in the disk is so high that dust collides and grows larger. Therefore, the growth of dust particles in the disk around DM Tau would occur because the β index obtained from millimeter and submillimeter continuum flux is much smaller than 2.

3.4. *Comparison with the Results from the* 45 m *Telescope*

Using the Nobeyama 45 m telescope, Handa et al. (1995) observed DM Tau in the ^{12}CO (1–0), ^{13}CO (1–0), and C^{18}O

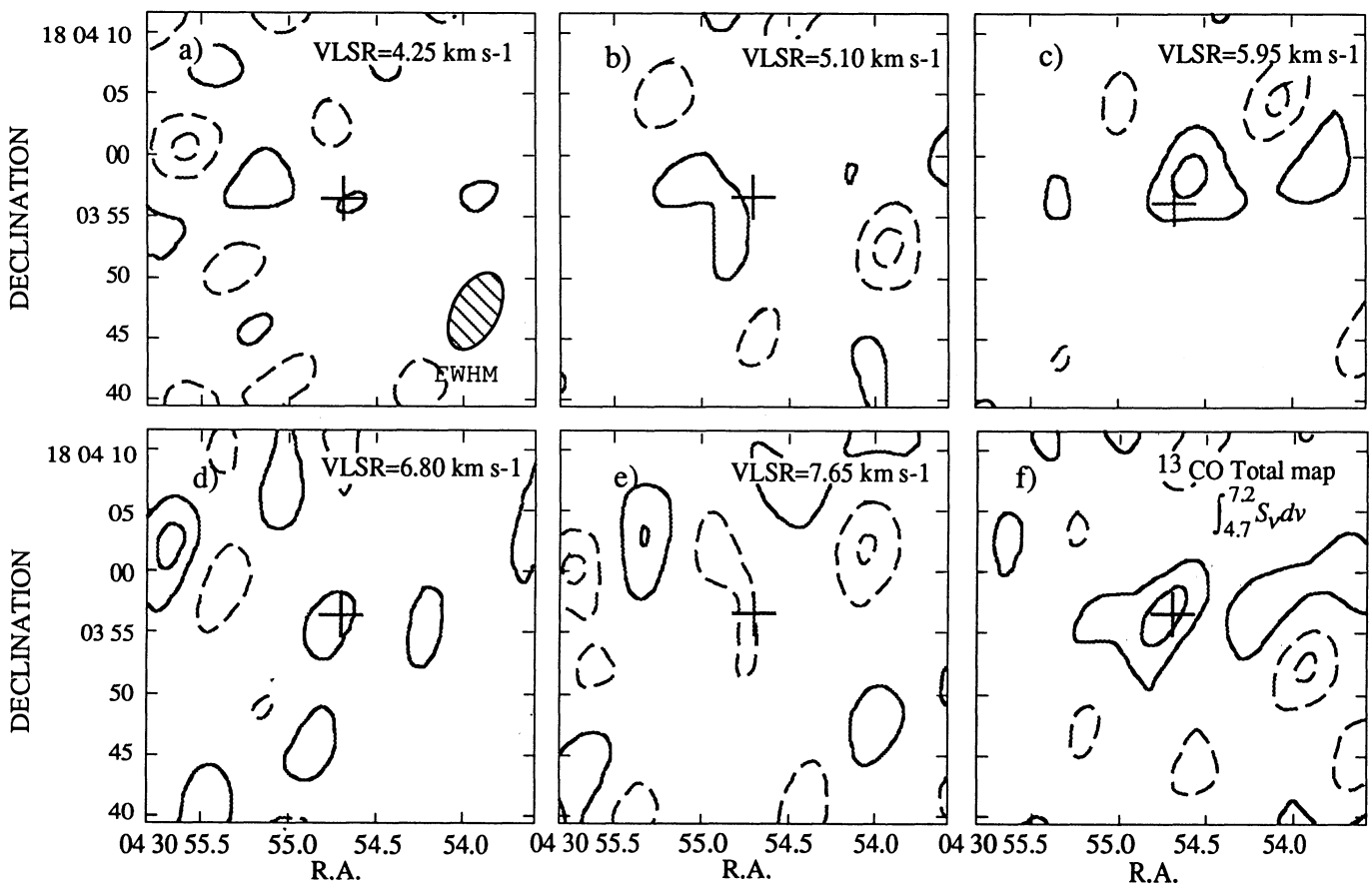

FIG. 3.—(*a–e*) Velocity channel maps of ^{13}CO emission of DM Tau for velocity over V_{LSR} = 4.3–7.7 km s^{-1}. The center velocity of each channel with a 0.85 km s^{-1} width is shown in each panel. A cross indicates the stellar position. The contour interval is 330 mJy beam^{-1} (1.5 σ contour). A contour with a negative level is indicated with a dashed line. (*f*) A map of total integrated ^{13}CO emission over V_{LSR} = 5.1–6.8 km s^{-1} (*b–d*). The contour interval is 180 mJy beam^{-1}.

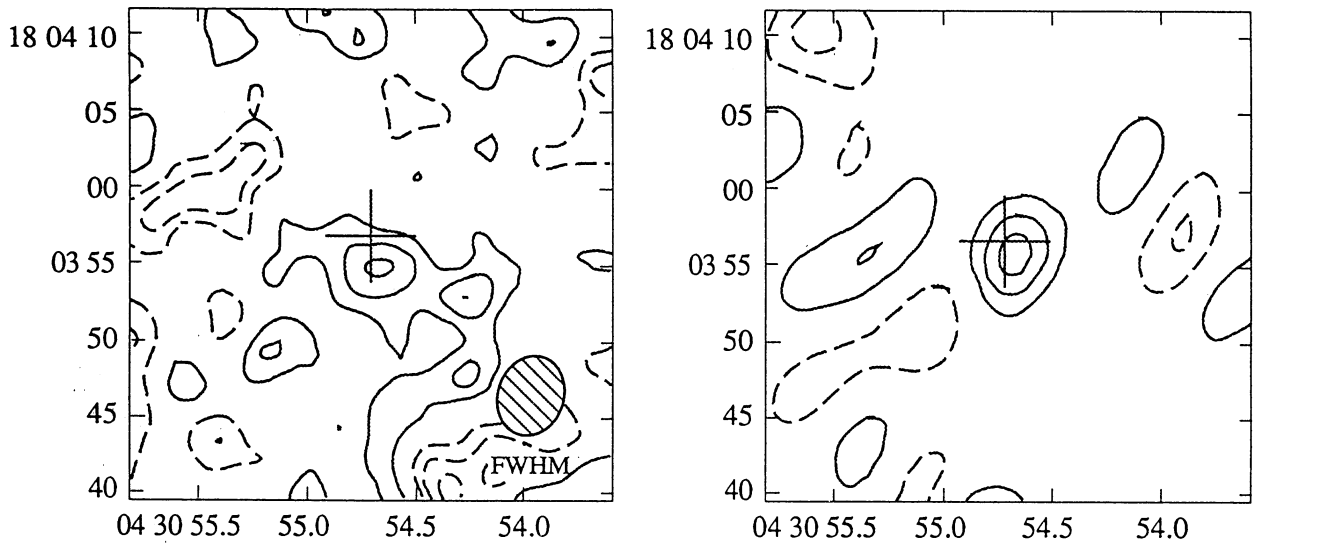

FIG. 4.—*Left:* A map of continuum emission at 2.6 mm taken with 5".7 × 4".2 resolution. The peak flux density in this map is 22 mJy per beam, and the integrated flux is 23 mJy. The contour level is 7 mJy beam^{-1}. *Right:* A map of continuum emission at 2.7 mm with 7".0 × 3".9 resolution; the peak flux density in this map is 27 mJy. The contour level is 8 mJy beam^{-1}.

(1–0) lines and revealed that ^{12}CO and ^{13}CO emission at $V_{LSR} \sim 6$ km s^{-1} was associated with the star. It is remarkable that the obtained ^{13}CO spectrum shows the double-peaked structure which is expected from the Keplerian motion of the gas disk (Omodaka, Kitamura, & Kawazoe 1992; Skrutskie et al. 1993). However, no C^{18}O emission was detected. In this section we compare our results with those from the 45 m telescope.

The ^{12}CO spectrum obtained by Handa et al. (1995) has a line width of 1.7 km s^{-1} and is centered at $V_{LSR} = 5.9$ km s^{-1}. Our derived ^{12}CO line width, 1.6–3.2 km s^{-1}, is consistent with their value, 1.7 km s^{-1}. The total flux of the ^{12}CO emission is obtained to be 1.85 Jy km s^{-1}, and the total flux of the ^{13}CO emission is obtained to be 0.78 Jy km s^{-1}. Our observation with the NMA shows that the derived total ^{12}CO flux is 4.8 Jy km s^{-1} and the total ^{13}CO flux is 1.5 Jy km s^{-1}. Derived total fluxes of ^{12}CO and ^{13}CO with the NMA are larger than those obtained with the 45 m telescope. This discrepancy is large even if we consider the flux uncertainties of the NMA and the 45 m telescope. The source coupling factor of the 45 m telescope (less than one for such a extended structure) or the pointing error of the 45 m telescope might be responsible for the discrepancy. The discussion in the next section, however, essentially will not change. In addition, the ratio of total integrated ^{12}CO intensity to total integrated ^{13}CO intensity derived with the 45 m telescope, 0.42, is consistent with our value, 0.3 ± 0.15.

4. DISCUSSION

4.1. *Size and Velocity Structure of Circumstellar Gas Disk around DM Tau*

It is important to investigate the kinematics and structures of the circumstellar gas disks associated with low-mass stars to understand the planet formation occurring around them. We detected significant ^{12}CO, ^{13}CO, 2.6 mm, and 2.7 mm continuum emissions just toward the young star DM Tau as described in the previous section. ^{12}CO channel maps show the systematic velocity gradient along the major axis of the disk, which indicates the existence of a rotating disk around DM Tau. We estimate the radius and inclination of the disk in this section. The mass of the disk is estimated in § 4.2.

The radius of the disk is estimated to be 300–350 AU by the separation of the peaks of the blue- and redshifted emissions (Figs. 1*b*, 1*e*, and 2*b*), and the line-of-sight rotational velocity is 0.6 km s^{-1} from the mean of V_{LSR} weighted by the ^{12}CO intensity on the blue and red components. The existence of the clear ^{12}CO velocity structure indicates that the disk orientation is not face on. On the other hand, the disk appears to be not edge on but nearly face on because the integrated map shows that ^{12}CO emission is extended along the minor axis and that its size is comparable to that along the major axis. Therefore, the inclination of the disk would be smaller than 45° (inclination is 0° for face-on). The obtained line of velocity, 0.60 km s^{-1}, is roughly consistent with the line-of-sight velocity of Keplerian rotation at $r = 350$ AU, 0.70 km s^{-1} which is estimated assuming $i = 40°$. Figure 5*a* shows an observed ^{12}CO position-velocity diagram along the major axis of the disk at P.A. = 160°. It seems that the disk has a rigid rotation and not a Keplerian rotation; however, this is not real, but an effect of finite spatial and velocity resolutions as discussed so far (e.g., Richer & Padman 1991; Dutrey et al. 1994). In such a case as the finite resolution, the direct comparison between the position-velocity diagram and the Keplerian rotation curve is difficult, and the position-velocity diagram can agree only in the fainter parts of the diagram at higher velocities (Richer & Padman 1991). Consequently, the obtained position-velocity diagram would be consistent with the Keplerian rotation of the disk in DM Tau. The disk parameters estimated above have some uncertainty because of the finite spatial and velocity resolution of our observations.

We have performed a calculation of the position-velocity diagram for a Keplerian disk model and compared it with the observed one. Figure 5*b* shows a position-velocity diagram calculated by taking into account ^{12}CO line radiative transfer for a Keplerian disk model that is based on the Kyoto model (for details, see Omodaka et al. 1992; Kitamura et al. 1993). For the calculation, we used the radius of 350 AU, the inclina-

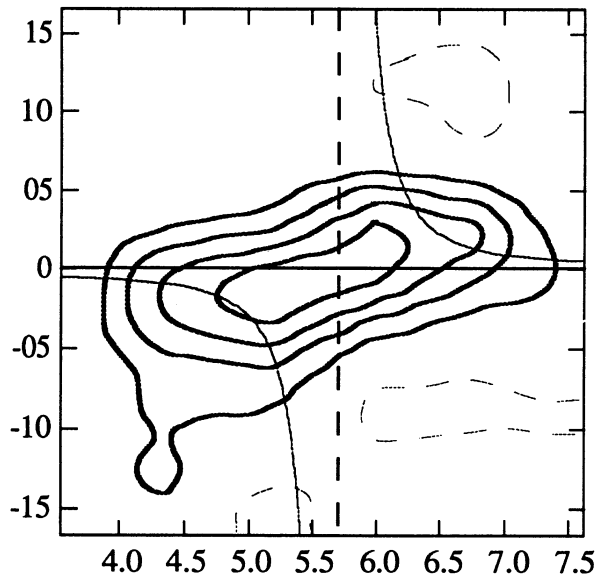

FIG. 5a

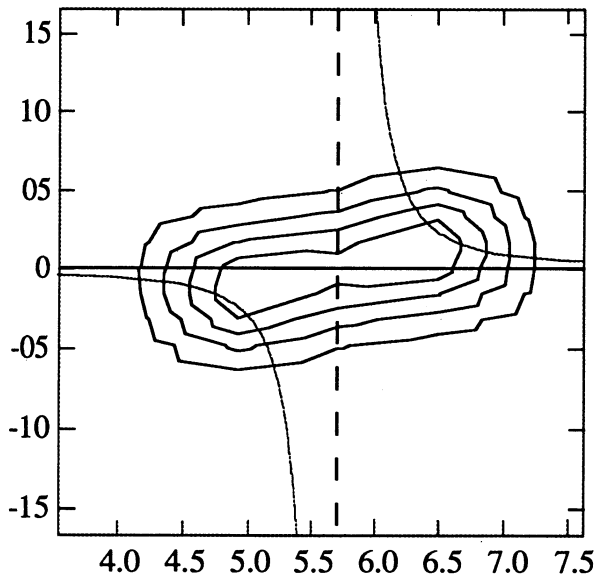

FIG. 5b

FIG. 5.—(*a*) Observed ^{12}CO position-velocity map across the major axis at P.A. = 160° is shown. The velocity resolution is 0.81 km s^{-1}. The curve is a theoretical Keplerian rotation curve for 0.48 $M_\odot$ and 40° inclination. The contour interval is 270 mJy beam^{-1}. (*b*) Calculated position-velocity map of the ^{12}CO for the disk model with T_d = 15 K at 350 AU and M_* = 0.48 $M_\odot$. The inclination is 40°. The contour interval is 135 mJy beam^{-1}.

tion of 40°, the disk temperature of 15 K at 350 AU, a gas surface density proportional to $r^{-1.5}$, and the same beam size and velocity resolution as those in our observations. The observed position-velocity map was roughly reproduced by the model calculation, and it was confirmed that the estimated disk parameters would be reliable and consistent with those expected from the Keplerian disk with a radius of 350 AU around DM Tau. It should be noted that the absolute flux obtained from observations is larger than that from the model by a factor of 2; this discrepancy may be caused by the uncertainties of both disk parameters of the model and the flux of NMA.

4.2. *Estimation of Disk Mass*

The lower limit of the H_2 mass of the gas disk is estimated from the total flux density of the ^{13}CO emission by the following equation if we assume that the ^{13}CO emission is optically thin:

$$M(\mathrm{H_2}) = 3.18 \times 10^{-5}\, M_\odot \left(\frac{T_{ex} + 0.88\ \mathrm{K}}{1\ \mathrm{K}}\right) e^{5.29\ \mathrm{K}/T_{ex}} \times \left(\frac{D}{100\ \mathrm{pc}}\right)^2 \left[\frac{10^{-6}}{X(^{13}\mathrm{CO})}\right] \left(\frac{\int S_\nu\, dv}{\mathrm{Jy\ km\ s^{-1}}}\right), \quad (1)$$

where T_{ex} is the excitation temperature of ^{13}CO, D is the distance to DM Tau, S_ν is the total ^{13}CO flux density, and X (^{13}CO) is the fractional ^{13}CO abundance relative to H_2 (e.g., HOM). The obtained total ^{13}CO flux, $\int S_\nu dv$, is 1.5 Jy km s^{-1}. In order to calculate the mass of the disk using equation (1), we must estimate the excitation temperature, T_{ex}. Here we find only that T_{ex} must be much higher than 7 K (see § 3.1) considering the beam dilution effect and cosmic-ray heating, but we cannot estimate the precise value of T_{ex}. In this paper we adopt T_{ex} to be 15 K, this is almost the same value as that used in Kitamura et al. (1995a) for DM Tau. As a result, the lower limit of the H_2 mass is 1.9 × 10^{-3} $M_\odot$.

The optical depth of ^{13}CO, τ_{13}, is estimated to be roughly 0.4 ± 0.15 from the total flux ratio of ^{13}CO to ^{12}CO ~ 0.3 ± 0.15 (§ 3.2). It is necessary to correct the lower mass by a factor 1.2 ± 0.1 by taking into account τ_{13}, and consequently the H_2 mass of the disk is obtained to be 2.3 × 10^{-3} $M_\odot$.

The mass of the circumstellar disk (especially $r \leq 100$ AU ~ 0".7 at Taurus) is a very important parameter in order to decide the theory of planet formation. It should be noted, however, that the derived mass from the ^{13}CO flux is not for the inner region ($r \leq 100$ AU) but for the outer region ($r \geq 100$ AU) of the circumstellar disk around DM Tau. It is clear from the ^{13}CO observations that the detected velocity coverage at 1.5 σ level in ^{13}CO channel maps, 1.3 km s^{-1}, is comparable to a line-of sight rotation velocity at r = 100 AU, 1.3 km s^{-1}, expected from the Keplerian disk with a central mass of 0.48 $M_\odot$, and i = 40°. Thus, our ^{13}CO observations does not trace the inner region ($r \leq 100$ AU) with a line-of-sight rotational velocity larger than 1.3 km s^{-1} (cf. Handa et al. 1995).

The millimeter continuum emission probably arises not from free-free emission but from thermal emission of circumstellar dust in the inner region with a radius smaller than 100 AU (BSCG; Ander & Montmerle 1994). Therefore, it is possible to estimate the H_2 mass of the inner region. The mass of the disk around DM Tau is estimated to be 0.034 $M_\odot$ from 1.3 mm continuum emission by BSCG. We detected 2.6 mm continuum emission just toward DM Tau, and it is also possible to estimate the mass of the circumstellar disk assuming that the 2.6 mm emission is also optically thin and using an isothermal disk model (see Appendix in OKHI). The disk of DM Tau must be optically thin at 2.6 mm because the expected flux of an optically thick disk with a radius of 100 AU and with a temperature of 30 K is about 300 mJy, which is much larger than the observed one. Following the same method as OKHI, the H_2 mass of the disk is obtained to be 0.019 ± 0.006 $M_\odot$ using a total 2.6 mm continuum flux of ~23 ± 7 mJy, $\kappa_{2.6}$ = 0.01 cm^2 g^{-1}, and T_d = 30 K. This value is roughly consistent

with that estimated by BSCG taking into account errors introduced by the assumption of an isothermal disk and κ_ν (Andre & Montmerle 1994). It should be noted that if the surface density of the disk goes as $\Sigma(r) \propto r^{-p}$ and $M_d = 0.02\ M_\odot$ ($0.01 < r < 100$ AU), opacity at 2.6 mm is estimated to be larger than unity inside $r = 6$ AU for $p = 1.5$ and 2. Therefore, the mass derived from the 2.6 mm flux density in the inner region will be underestimated by a factor of about 1.3 and 2 for $p = 1.5$ and 2, respectively.

4.3. *The Radial Dependence of Surface Density*

In the last section, it is shown that ^{13}CO observation samples the outer region (100 AU $< r <$ 350 AU) and 2.6 mm observation samples the inner region ($r <$ 100 AU). Using the outer and inner masses of the disk, it is possible to impose a restriction on the radial dependence of gas surface density, $\Sigma(r)$, in the circumstellar disk. In the following calculation, we assume that $\Sigma(r)$ is proportional to r^{-p} from the inner to the outer region. The mass of the inner (0.01 AU $\leq r \leq$ 100 AU) and outer region (100 AU $\leq r \leq$ 350 AU) can be written in the following equations:

$$M_{\rm out} = \sum_{100\ {\rm AU}} \int_{100\ {\rm AU}}^{350\ {\rm AU}} r^{-p} 2\pi r\, dr\ , \tag{2}$$

$$M_{\rm in} = \sum_{100\ {\rm AU}} \int_{0.01\ {\rm AU}}^{100\ {\rm AU}} r^{-p} 2\pi r\, dr\ . \tag{3}$$

By combining these two equations, we obtain the mass ratio

$$M_{\rm out}/M_{\rm in} = \int_{100\ {\rm AU}}^{350\ {\rm AU}} r^{-p} 2\pi r\, dr \Big/ \int_{0.01\ {\rm AU}}^{100\ {\rm AU}} r^{-p} 2\pi r\, dr\ . \tag{4}$$

Using $M_{\rm out} = 2.3 \times 10^{-3}\ M_\odot$ from ^{13}CO and $M_{\rm in} = 0.019 \pm 0.006\ M_\odot$ from 2.6 mm, the mass ratio is 8.3 ± 2. In the case of $M_{\rm in} = 0.034\ M_\odot$ obtained by BSCG, the mass ratio is 14.8. Considering these mass ratios and equation (4), the index p of the disk around DM Tau is estimated to be 2.0 ± 0.1 and 2.1 ± 0.1, respectively. It should be noted that the mass ratio has a larger uncertainty because the $M_{\rm in}$ has large uncertainty as a result of $\kappa_{2.6}$. In the case of $\kappa_{2.6}$ with a uncertainty of an order, that is, $M_{\rm in}$ ranging from 0.006(0.019/3) to 0.102(0.034 × 3) $M_\odot$, the mass ratio is ranging from 2.8(8.3/3) to 44.4(14.8 × 3), which gives $p = 2.0 \pm 0.3$. This value is still significantly larger than the 1.5 predicted by the Kyoto model and assumed by BSCG.

Gaseous CO molecules will be converted to solid CO for temperatures lower than 13–16 K, and most CO might be in solid form in the outer cold region at 350 AU (Kawabe et al. 1993). If the depletion of ^{13}CO occurs in the outer cold region, we underestimated the mass of the outer region. In such a case the index, p, is expected to be smaller than 2.0.

4.4. *The Circumstellar Gas disk around DM Tau*

The rotating gaseous disk around DM Tau has a similar size to that around GG Tau with a mass of 0.28 $M_\odot$ and an age of 4.3×10^4 yr (Handa et al. 1995). GG Tau is a binary system, and the circumstellar gas disk is a ring structure revealed by Dutrey et al. (1994). GG Tau, however, has a near-infrared (NIR) excess, and each star is expected to have a small dust disk with a radius of about 10 AU. DM Tau has been reported not to be a binary system, in which case DM Tau would be a single star (Leinert et al. 1993). The gas structure around DM Tau would not have the inner hole caused by the perturbation of the binary rotation like GG Tau. From our observation, even in a single star we find the existence of the outer structure of the gas disk ($r >$ 100 AU) which is larger than our solar system. This fact indicates that such a large disk is intrinsic.

Although the disk around DM Tau is larger than the solar system, the rotating gaseous disk may be a protoplanetary disk predicted theoretically because the mass of the disk is estimated to be 0.04 $M_\odot$ by summing up masses of the inner (0.034 $M_\odot$ by BSCG) and outer ($2.3 \times 10^{-3}\ M_\odot$) regions, and this mass is comparable to the value required for a minimum solar nebula ($M_d \sim 0.01\ M_\odot$). Around DM Tau, there does not exist a 1000 AU scale massive envelope which is similar to a dynamically accreting disk structure in HL Tau (HOM) or to a dispersing disklike structure around DG Tau (Kitamura, Kawabe, & Saito 1995b). This means that a protoplanetary gas disk survives around the star even after the dissipation of the envelope, at least for $\sim 10^6$ yr. In addition to the existence of the protoplanetary disk, the other remarkable feature of DM Tau is that the observed low values of the NIR flux (2.2 μm–12 μm) may result from a disk clearing by planet formation (Marsh & Mahoney 1992). But it is possible to explain such a spectral dip by a residual optically thin dust shell (Mathieu, Adams, & Latham 1991) or by the combined effects of dust grain opacity and vertical disk structure (Boss & Yorke 1993). We cannot conclude whether the planetary system is forming inside the protoplanetary gas disk or not because our observation does not give us the information of this region.

4.5. *Systemic Velocities and Orientations of Circumstellar Disks in the L1551 Region*

DM Tau is one of the T Tauri stars located in the L1551 region centered on a protostar L1551–IRS 5. GG Tau and HL Tau, which are reported to have circumstellar gas disks or disklike infalling envelopes, are also located in the L1551 region. We consider the relation of the circumstellar gas disks in this region because they are very interesting from the viewpoint of formation mechanisms of these disks from molecular cloud cores.

Figure 6 shows orientations of the gas disks or disklike structure found around DM Tau, GG Tau, HL Tau, and L1551–IRS 5 together with the systemic velocities of the gas disks. These systemic velocities are consistent with the stellar velocities obtained from optical data within error bars (Jones & Herbig 1979; Hartmann et al. 1986). It is remarkable that the systemic velocities are found in the narrow range of $V_{\rm LSR} =$ 5.7–6.4 km s^{-1}. This fact suggests that these stars in the L1551 region were formed in the same parent cloud and the difference among these systemic velocities might be originated from turbulent velocities in the cloud.

It can be seen that gas disks of three young stars and a protostar (DM Tau, HL Tau, GG Tau, and L1551–IRS 5) have nearly the same P.A. of the major axes of the disks, 125°–160°, although optical jets in the HL/XZ Tau region are not parallel to each other (Mundt, Ray, & Bührke 1988). The projected direction of the magnetic field in this region was measured with the observations of optical polarization (Vrba, Strom, & Strom 1976), and the P.A. of the magnetic field was found to be about 70° (dashed square in Fig. 6). The major axes of the disks in the L1551 region are almost perpendicular to the magnetic field. If we consider that these stars were formed in the same parent cloud, it is possible to speculate the following scenario about the formation of young stars in L1551 region (e.g., Black & Scott 1982). The parent cloud with magnetic field (P.A. ~ 70°) might fragment into several dense cloud cores, and velocity

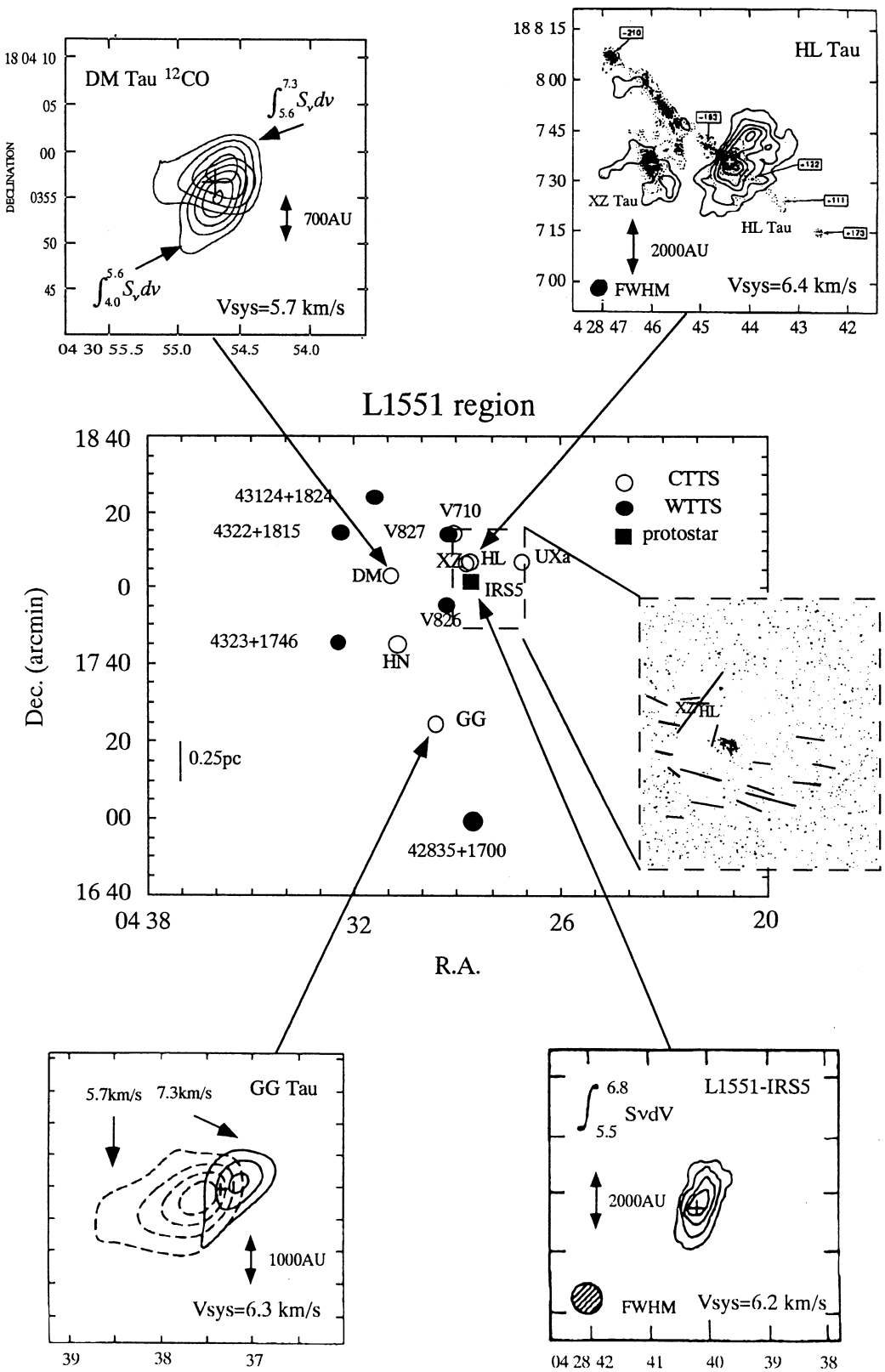

FIG. 6.—The distribution of young stars in the L1551 cloud. Open circles represent classical T Tauri stars (CTTSs), and filled circles represent weak line T Tauri stars (WTTS's). The square represents the protostar. The maps of gas disks are shown with DM Tau, GG Tau, HL Tau, and L1551–IRS 5 (this work; Kawabe et al. 1993; HOM; Sargent et al. 1988). The orientation of the magnetic field by the optical polarimetry observation is also shown as indicated in the dashed square (Vrba et al. 1976).

differences among them are of the order of 1 km s^{-1}. In the course of formation of protostars and T Tauri stars from cores, the component of the angular momentum perpendicular to the magnetic field in each core was transferred to the outer region by magnetic braking, and as a result the circumstellar disk, which is supported by remained angular momentum, is aligned. We should investigate the fine structure of the magnetic field and more samples in order to confirm the above scenario because we currently have small samples of a star with a gas disk in this region.

We would like to thank the referee for his comments and suggestions and Stephen E. Strom, Ronald L. Snell, and Michael F. Skrutskie for useful discussions. We also thank the staff at Nobeyama Radio Observatory for their operation of the NMA.

REFERENCES

Adams, R. C., Emerson, J. P., & Fuller, G. A. 1990, ApJ, 357, 606
Andre, Ph., & Montmerle, T. 1994, ApJ, 420, 837
Beckwith, S. V. W., & Sargent, A. I. 1991, ApJ, 381, 250
Beckwith, S. V. W., Sargent, A. I., Chini, R. S., & Gusten, R. 1990, AJ, 99, 924 (BSCG)
Black, D. C., & Scott, E. H. 1982, ApJ, 263, 696
Boss, A. P., & Yorke, H. W. 1993, ApJ, 411, L99
Cameron, A. G. W. 1985, in Protostars & Planets II, ed. D. C. Black & M. S. Matthews (Tucson: Univ. Arizona Press), 1073
Chikada, Y., et al. 1987, Proc. IEEE, 75, 1203
Cohen, M., Emerson, J. P., & Beichman, C. A. 1989, ApJ, 339, 455
Dutrey, A., Guilloteau, S., & Simon, M. 1994, A&A, 286, 149
Elias, J. H. 1978, ApJ, 224, 857
Handa, T., et al. 1995, ApJ, 449, 894
Hartmann, L., Hewett, R., Stahler, S., & Mathieu, R. D. 1986, ApJ, 309, 275
Hayashi, C., Nakazawa, K., & Nakagawa, Y. 1985, in Protostars & Planets II, ed. D. C. Black & M. S. Matthews (Tucson: Univ. Arizona Press),1171
Hayashi, M., Ohashi, N., & Miyama, S. M. 1993, ApJ, 418, L71 (HOM)
Henning, Th., Pfau, W., Zinnecker, H., & Prusti, T. 1993, A&A, 276, 129
Herbig, G. H., & Robbin-Bell, K. 1988, Lick Obs. Bull, No. 1111
Jones, B. F., & Herbig, G. H. 1979, AJ, 84, 1872
Kawabe, R., Ishiguro, M., Omodaka, T., Kitamura, Y., & Miyama, S. M. 1993, ApJ, 404, L63
Kitamura, Y., Kawabe, R., & Saito, M. 1995b, ApJ, submitted
Kitamura, Y., Omodaka, T., Kawabe, R., Yamashita, T., & Handa, T. 1993, PASJ, 45, L27
Kitamura, Y., et al. 1995a, in preparation
Koerner, D. W., Sargent, A. I., & Beckwith, S. V. W. 1993, Icarus, 106, 1
Leinert, Ch., Zinnecker, H., Weitzel, N., Christou, J., Ridgway, S. T., Jameson, R., Haas, M., & Lenzen, R. 1993, A&A, 278, 129
Marsh, K. A., & Mahoney, M. J. 1992, ApJ, 395, L115
Mathieu, R. D., Adams, F. C., & Latham, D. W. 1991, AJ, 101, 2184
Miyake, K., & Nakagawa, Y. 1993, Icarus, 106, 20
Miyama, S. M., et al. 1995, in preparation
Mundt, R., Ray, T. P., & Bührke, T. 1988, ApJ, 333, L69
Ohashi, N., Kawabe, R., Hayashi, M., & Ishiguro, M. 1991, AJ, 102, 2054 (OKHI)
Omodaka, T., Kitamura, Y., & Kawazoe, E. 1992, ApJ, 396, 987
Richer, J. S., & Padman, R. 1991, MNRAS, 251, 707
Rucinski, S. M. 1985, AJ, 2321
Safronov, V. S., & Ruzmaikina, T. V. 1985, in Protostars & Planets II, ed. D. C. Black & M. S. Matthews (Tucson: Univ. Arizona Press), 959
Sargent, A. I., & Beckwith, S. V. W. 1989, in IAU Colloq. 120, Structure and Dynamics of the Interstellar Medium, ed. G. Tenorio-Tagle, M. Moles, & J. Melnick (Berlin: Springer), 215
———. 1991, ApJ, 382, L31
Sargent, A. I., Beckwith, S. V. W., Keene, J., & Masson, C. 1988, ApJ, 303, 416
Skrutskie, M. F., et al. 1993, ApJ, 409, 422
Strom, K. M., Strom, S. E., Edwards, S., Carit, S., & Skrutskie, M. 1989, AJ, 97, 1451
Sunada, K., Kawabe, R., & Inatani, J. 1993, Int. J. Infrared Millimeter Waves, 14, 1251
Vrba, F. J., Strom, S. E., & Strom, K. M. 1976, AJ, 81, 958